Clays and Clay Minerals, Vol. 45, No. 2, 290–294, 1997.

A NEUTRON DIFFRACTION STUDY OF INTERLAYER WATER IN SODIUM WYOMING MONTMORILLONITE USING A NOVEL DIFFERENCE METHOD

D. HUGH POWELL,[1] KOWUT TONGKHAO,[1] SHANE J. KENNEDY[2] AND PHILLIP G. SLADE[3]

[1] Department of Chemistry, University of Adelaide, South Australia 5005, Australia

[2] Australian Nuclear Science & Technology Organisation, Menai, New South Wales 2234, Australia

[3] CSIRO Division of Soils, Glen Osmond, South Australia 5064, Australia

Key Words—Interlayer, Montmorillonite, Neutron Diffraction, Structure, Water.

INTRODUCTION

The structure of the interlayer region of smectite clays is one of the fundamental problems of clay science. There have recently been considerable advances in the use of Monte Carlo computer simulations to study interlayer structure in both smectites and vermiculites (Boek et al. 1995; Chang et al. 1995; Skipper, Sposito and Chang 1995; Karaborni et al. 1996). In the case of vermiculites, these studies have been backed up with neutron diffraction studies (Skipper et al. 1991, 1994; Skipper, Smalley et al. 1995). Neutron diffraction is a powerful technique for the study of multicomponent systems, because the technique of isotopic substitution can be used to separate individual correlation functions from the overall diffraction pattern. The fact that vermiculites form well-defined macroscopic crystals allows accurate sample orientation, so that scattering density profiles across the interlayer region perpendicular to the clay layers can be obtained, and detailed models of the interlayer structure constructed. The relatively disordered structure of the montmorillonites, with crystallites less than 20 μm in diameter, makes them difficult to study using such an approach. However, their technological and environmental importance make it highly desirable to obtain experimental structural information that can be used to test the validity of simulation results. Early neutron diffraction studies suggested that at least a component of the diffraction from the interlayer is liquid-like (Hawkins and Egelstaff 1980). We present an approximate difference method, using the dehydrated clay as a reference system, that allows us to isolate this liquid-type diffraction and hence obtain normalized radial distribution functions. The functions confirm the disordered nature of the interlayer region and can be used as a critical test of simulation results.

EXPERIMENTAL

The montmorillonite sample (SWy-2, Crook County, Wyoming) was washed 5 times with 1 *M* NaCl, then washed free of Cl^- by dialysis, using the $AgNO_3$ test. The <2 μm fraction was selected by sedimentation. The Na-montmorillonite was dried using a rotary evaporator, then lightly crushed in a mortar and pestle before final dehydration under vacuum at 110 °C. The composition of the resulting sample was checked by X-ray diffraction (XRD) of a pressed powder sample and a partially oriented, ethylene glycol-saturated sample. The only significant impurity found was about 1–2% quartz. The sample was rehydrated with D_2O by exposure to a D_2O atmosphere, then redried under vacuum at 110 °C. No attempt was made to replace the lattice hydroxyl protons with deuterium, as rather severe conditions are required (Hawkins and Egelstaff 1980). The dehydrated sample was transferred to the sample container in a dry glove bag. A portion of the dehydrated sample was exposed to a D_2O atmosphere in a desiccator prior to transfer to the sample container in a D_2O-saturated glove bag (D_2O is preferred to H_2O in neutron diffraction experiments because hydrogen has a large incoherent scattering cross section). The sample container was a 5 cm high, 12.5 mm od, 12.1 mm id vanadium cylinder closed with a stainless steel cap and rubber O-ring. For both samples, the filled sample container was weighed before and after the experiment to check that no hydration or dehydration of the sample had occurred. The D_2O content of the hydrated sample was found gravimetrically to be 205 ± 5 mg g^{-1}, corresponding to the 2-layer hydrate. Chemical analyses of Wyoming-type montmorillonites are given by Newman (1987) and Slade et al (1991). In order to simplify the analysis, we assumed the idealized formula $Na_{0.75}(Si_{7.75}Al_{0.25})(Al_{3.5}\ Mg_{0.5})O_{20}(OH)_4$ for the dry Na--saturated clay: the fact that we neglect the presence of Fe and other contaminants does not have a significant effect on the calculated scattering properties. From our gravimetric analysis, the water content of the 2-layer hydrate was 9.5 D_2O per formula unit, as above.

The diffraction patterns at ambient temperature (298 K) of the dehydrated and hydrated (D_2O) samples, the empty sample container, the instrument background and a 13-mm diameter rod were measured on the me-

https://doi.org/10.1346/CCMN.1997.0450217 Published online by Cambridge University Press

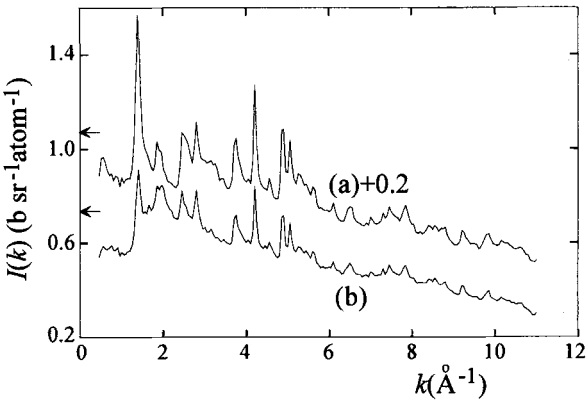

Figure 1. Corrected and normalized neutron diffraction patterns obtained for Na-montmorillonite (a) in the dried state and (b) in the 2-layer hydrate (D_2O). The horizontal arrows indicate the predicted values of the self-scattering term in Equation [1].

dium-resolution power diffractometer (MRPD) at the steady-state high-flux Australian reactor (HIFAR) facility of the Lucas Heights Research Laboratories. The instrument wavelength was 1.057(2) Å, and the 24-element multiple angle detector was stepped at 0.1° intervals covering 0 to 138°. The raw data were corrected for contributions due to background, empty container, attenuation and multiple scattering, and were normalized with respect to the scattering from the vanadium rod (Paalman and Pings 1962; Blech and Averbach 1965; North et al. 1968). In these corrections, the attenuation coefficients of the samples were calculated using the weighed quantity of sample, the known volume of the sample container and the mean scattering and absorption cross sections of the samples. While the published bound scattering cross sections and absorption cross sections (Sears 1992) are adequate for the majority of elements, the effective scattering cross sections for D in interlayer D_2O and H in the clay hydroxyl groups can be expected to deviate quite significantly from their bound values. On the basis of the total cross sections of D_2O and H_2O (Hughes and Harvey 1955), effective scattering cross sections of 3.35 b and 35 b respectively were assigned to D and H. The calculated scattering and absorption cross sections at the incident wavelength were 6.58 b and 0.10 b for the dry clay and 5.59 b and 0.06 b for the 2-layer hydrate (1 barn, b = 100 fm^2).

RESULTS AND DISCUSSION

The corrected and normalized diffraction intensities, $I(k)$, for the dehydrated clay (top trace) and the 2-layer hydrate (bottom trace) are shown in Figure 1. Within the static approximation, these intensities are given by:

$$I(k) = \sum_{\alpha} c_{\alpha}\overline{b_{\alpha}^2} + F(k) \qquad [1]$$

where c_α is the atomic fraction and $\overline{b_\alpha^2}$ the mean square scattering length of species α and the scattering factor, $F(k)$ will be a combination of clay-clay, clay-water and water-water terms. The calculated values of the self-scattering terms, or first term in Equation [1], for the 2 samples are shown as horizontal arrows in Figure 1. The fact that the $I(k)$ tend toward these values at low k is an indication that the normalization of the data is correct. The data for the dry clay slope downwards with increasing k due to inelastic scattering from the hydroxyl protons. The slope on the data for the 2-layer hydrate is due to a combination of the hydroxyl protons and the slope due to inelastic scattering from D_2O, as found in aqueous systems.

The pattern of Bragg peaks due to the quasi-crystalline structure of the clays is similar for the 2 samples. For the 2-layer hydrate, there is an additional diffuse diffraction pattern superimposed on Bragg peaks. In addition, the Bragg peaks are of lower intensity for this sample. We propose that the Bragg scattering results essentially from the clay structure, while the diffuse scattering is due to the liquid-like structure of the interlayer and thus arises from clay-interlayer and interlayer-interlayer type interactions. If one assumes that the clay structure is essentially unchanged upon hydration, the Bragg diffraction pattern will be identical for the 2 samples, except that it will be lower in the $I(k)$ for the 2-layer hydrate due to the lower atomic fraction of the clay. One can then construct the difference function defined by:

$$\Delta(k) = I'(k) - \frac{c'_{Si}}{c_{Si}} I(k)$$
$$= \sum_{\alpha} c_{\alpha}\overline{b_{\alpha}^2} + \sum_{\alpha}\sum_{\beta} c_{\alpha}c_{\beta}b_{\alpha}b_{\beta}[S_{\alpha\beta}(k) - 1] \qquad [2]$$

where the primes refer to the hydrated sample. The atomic fraction of Si, c_{Si}, is proportional to the clay concentration; α now refers only to the interlayer water atoms (D and O in D_2O); and β refers to all atom types in both the interlayer water and the clay. The second term in Equation [2] is thus a sum of the water-clay and water-water partial structure factors, $S_{\alpha\beta}(k)$: within the approximation used, the clay diffraction pattern is eliminated. The values of the different prefactors $2c_\alpha c_\beta b_\alpha b_\beta$ (or $c_\alpha^2 b_\alpha^2$ for $\alpha = \beta$) and the self-scattering term are given in Table 1.

The difference function calculated according to Equation [2] is shown in Figure 2. It can be seen that the cancellation of the Bragg peaks in the difference is almost perfect, so that our assumption that the clay diffraction pattern is unchanged upon hydration is adequate for this practical purpose. The similarity of the general form of the difference function to the diffraction pattern of a salt solution in D_2O is striking, and indicates that at least part of the interlayer should be considered liquid (note that the ion-water correlations are negligibly small in both functions). The fact that

https://doi.org/10.1346/CCMN.1997.0450217 Published online by Cambridge University Press

Table 1. Scattering parameters in the difference functions, $\Delta(k)$ and $G(r)$ (all in units of barn: 1 b = 100 fm^2). The symbol O2 is used to designate oxygen in the aluminosilicate layer, as opposed to oxygen in interlayer water. All scattering lengths are taken from Sears (1992).

Water-water terms		
$c_D^2 b_D^2$	$2c_D c_O b_D b_O$	$c_O^2 b_O^2$
0.0335	0.0291	0.0063

Water-clay terms											
$2c_D c_{O2} b_D b_{O2}$	$2c_O c_{O2} b_O^2$	$2c_D c_{Si} b_D b_{Si}$	$2c_D c_H b_D b_H$	$2c_O c_{Si} b_O b_{Si}$	$2c_D c_{Al} b_D b_{Al}$	$2c_O c_H b_O b_H$	$2c_O c_{Al} b_O b_{Al}$	$2c_D c_{Na} b_D b_{Na}$	$2c_O c_{Na} b_O b_{Na}$	$2c_D c_{Mg} b_D b_{Mg}$	$2c_O c_{Mg} b_O b_{Mg}$
0.0736	0.0320	0.0170	−0.0079	0.0074	0.0068	−0.0034	0.0030	0.0014	0.0006	0.0014	0.0006

$$\text{Self scattering} = \sum_\alpha c_\alpha \overline{b_\alpha^2} \qquad 0.213$$

$$G(0) = -\sum_\alpha \sum_\beta c_\alpha c_\beta b_\alpha b_\beta \qquad -0.202$$

the diffraction pattern tends to oscillate around the calculated self-scattering term at low k indicates that the pattern originates from all the interlayer water. The downward slope of the data at high k-values is characteristic of inelasticity effects in self-scattering from light atoms (D in this case). We have adopted an empirical approach, based on the fact that the largest term in the inelasticity corrections should be proportional to k^2 (Montague et al 1981), in order to produce the corrected difference function in Figure 3.

Real space information was obtained from the Fourier transform of this corrected difference function via:

$$G(r) = \frac{1}{2\pi\rho_n}\int_0^\infty \left[\Delta(k) - \sum_\alpha c_\alpha \overline{b_\alpha^2}\right] k^2 \frac{\sin kr}{kr}\, dr$$

$$= \sum_\alpha \sum_\beta c_\alpha c_\beta b_\alpha b_\beta [g_{\alpha\beta}(r) - 1] \qquad [3]$$

where $G(r)$ is a sum of partial radial distribution functions, $g_{\alpha\beta}(r)$, weighted according to the scattering prefactors in Table 1. The atomic number density, ρ_n, was estimated to be 0.1 Å^{-3} on the basis of the unit-cell dimensions measured for Na-vermiculite (Slade et al. 1985). The $G(r)$ obtained is shown in Figure 4. Note that the criteria used in the empirical correction of $\Delta(k)$ were that $\Delta(k)$ should tend to the self-scattering term at high k, that $G(r)$ should tend to the value $G(0)$ (Table 1) at low r, and that high-frequency ripples in $G(r)$ should be minimized. The form of $G(r)$ was rather insensitive to the exact values used in the correction procedure, except at low r. Removing the apparent remnants of Bragg peaks in $\Delta(k)$ at approximately 1.5 and 2.8 Å^{-1} using a spline-fitting procedure had no discernable effect on the form of $G(r)$.

The first and most intense peak in $G(r)$ is due to the intramolecular O-D interaction. Because of the restricted k-range used for the experiments, this peak is considerably broadened and slightly shifted in r-space. However, the integral of this peak provides a check of the normalization of the data via:

$$n_O^D = 4\pi\rho_n c_D \int_{r_0}^{r_{min}} g_{OD}(r) r^2\, dr$$

$$\approx \frac{4\pi\rho_n}{2c_O b_O b_D}\int_{r_0}^{r_{min}} [G(r) - G(0)] r^2\, dr \qquad [4]$$

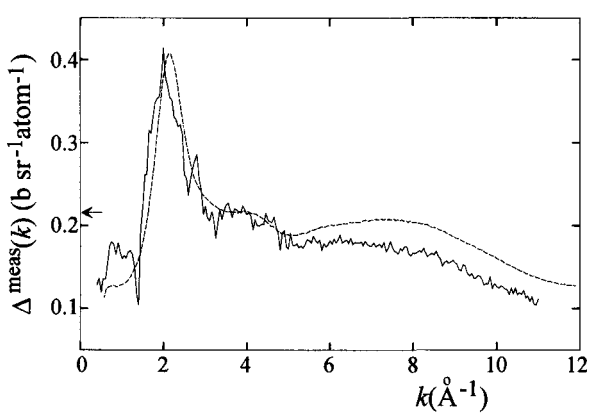

Figure 2. The difference function calculated directly from the experimental data using Equation [2] (full line) compared to the diffraction pattern obtained from a 2.0 mol kg^{-1} solution of $NiCl_2$ in D_2O (Powell et al. 1989) (dashed line). The horizontal arrow indicates the predicted self-scattering component in Equation [2].

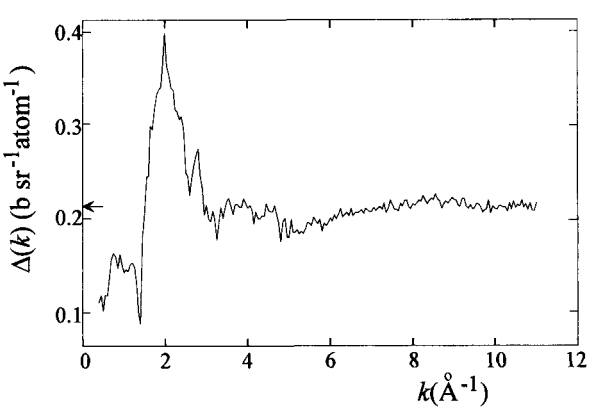

Figure 3. The empirically corrected difference function, $\Delta(k) = \Delta^{meas}(k) - 0.019 + 0.00102k^2$. The horizontal arrow indicates the predicted self-scattering component in Equation [2].

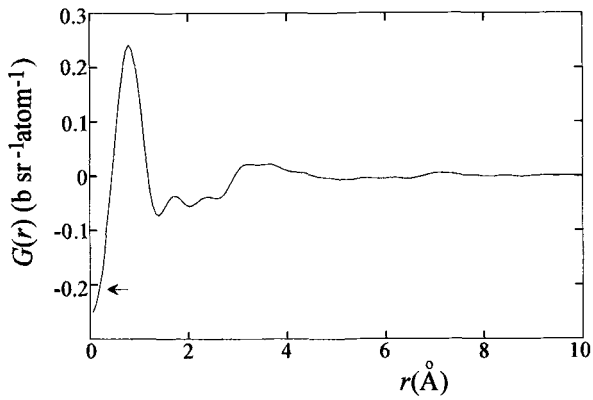

Figure 4. The Fourier transform, $G(r)$, of the empirically corrected difference function in Figure 3. The horizontal arrow corresponds to the predicted value of $G(0)$.

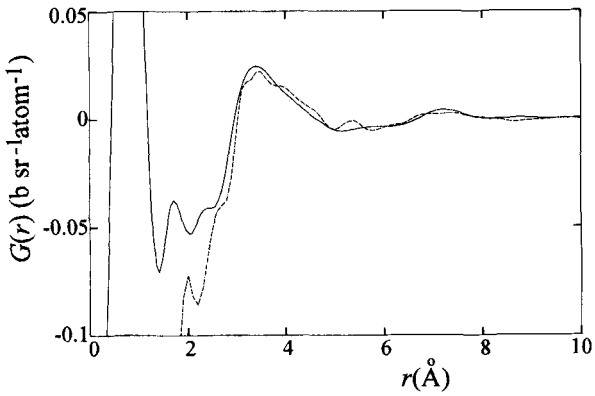

Figure 5. The experimental $G(r)$ (full line) compared to the function $2.43 \times [0.1028 g_{OH}(r) + 0.0384 g_{OO}(r) + 0.0335 g_{HH}(r) - 0.1747]$ for pure water (dashed line) calculated from the data of Soper and Phillips (1986) (the factor 2.43 takes account of the different atomic fractions of D and O in the clay and in pure water).

where n_O^D is the mean number of D-atoms within a distance r_{min} of a given O-atom, r_{min} is the minimum after the first peak in $G(r)$ and $G(0)$ is the low r limit of $G(r)$ given in Table 1. Appropriate integration of $G(r)$ yields a value $n_O^D = 2.8$, compared to the expected value of 2.0 for the water molecule. The observed discrepancy is probably due to the overlap of this broadened peak with succeeding peaks, including the intermolecular D-D peak. Nevertheless, the fact that a value near 2.0 is obtained is strong evidence that the majority of interlayer water molecules contribute to this liquid type diffraction pattern.

In Figure 5, we concentrate on the intermolecular part of $G(r)$, compared to an appropriately weighted combination of the experimental $g_{\alpha\beta}(r)$ for liquid water (Soper and Phillips 1986). Above 3 Å, the 2 sets of data are similar, indicating that the gross structural environment of water in the clay is similar to that in pure water. The differences in the position of the peak and shoulder between 1.5 and 3 Å, however, indicate significant perturbation of the hydrogen bonding network compared to bulk water, presumably due to interactions with interlayer ions and the clay surface (Sposito and Prost 1982). We reserve full interpretation of these features until we have completed further experiments, but we note that computer simulations (Chang et al. 1995) indicate that interlayer water does not replicate bulk structure or mobility, even in the 3-layer hydrate.

These results show that a simple differencing technique can be used to effectively isolate the liquid-type diffraction from the interlayer region of montmorillonite, and that the majority of interlayer water has a liquid-like structure. Thus, although analysis of X-ray band profiles (Méring and Brindley 1967) and an X-ray structural study of the interlayer region of a 2-layer hydrate of Na-vermiculite (Slade et al 1985) indicate some ordering of the interlayer water with respect to the clay surface, the interlayer water should certainly not be considered crystalline. The novel method presented creates the possibility of further experiments using isotopic substitution, both in the solvent and of interlayer ions, to resolve the different partial radial distribution functions and so to determine the extent of disruption of the water structure by interactions with the clay surface. These partial radial distribution functions will be a crucial test of the results of computer simulations and will be complementary to this rapidly developing field of study.

ACKNOWLEDGMENTS

This work was supported by the Australian Research Council (Grant 4003/95) and the Australian Institute of Nuclear Science and Engineering (Grant 95/065).

REFERENCES

Blech IA, Averbach BL. 1965. Multiple scattering of neutrons in vanadium and copper. Phys Rev 137:A1113–1116.

Boek ES, Coveney PV, Skipper NT. 1995. Monte Carlo molecular modeling studies of hydrated Li-, Na-, and K-smectites: Understanding the role of potassium as a clay swelling inhibitor. J Am Chem Soc 117:12608–12617.

Chang F-RC, Skipper NT, Sposito G. 1995. Computer simulation of interlayer molecular structure in sodium montmorillonite hydrates. Langmuir 11:2734–2741.

Hawkins RK, Egelstaff PA. 1980. Interfacial water structure in montmorillonite from neutron diffraction experiments. Clays Clay Miner 28:19–28.

Hughes DJ, Harvey JF. 1955. Neutron cross sections. New York: McGraw-Hill. 328 p.

Karaborni S, Smit B, Heidug W, Urai J, van Oort E. 1996. The swelling of clays: Molecular simulations of the hydration of montmorillonite. Science 271:1102–1104.

Méring J, Brindley GW. 1967. X-ray diffraction band profiles of montmorillonite—Influence of hydration and of the exchangeable cations. Clays Clay Miner 15:51–60.

Montague DG, Gibson IP, Dore JC. 1981. Structural studies of liquid alcohols by neutron diffraction: I. Deuterated methyl alcohol CD_3OD. Mol Phys 44:1355–1367.

Newman ACD. 1987. Chemistry of clays and clay minerals. London: Mineral Soc. 480 p.

North DM, Enderby JE, Egelstaff PA. 1968. The structure factor for liquid metals. I. The application of neutron diffraction techniques. J Phys C 1:784–794.

Paalman HH, Pings CJ. 1962. Numerical evaluation of X-ray absorption factors for cylindrical samples and annular cells. J Appl Phys 33:2635–2639.

Powell DH, Neilson GW, Enderby JE. 1989. A neutron diffraction study of $NiCl_2$ in D_2O and H_2O. A direct determination of $g_{NiH}(r)$. J Phys: Condens Matter 1:8721–8733.

Sears VF. 1992. Neutron scattering lengths and cross sections. Neutron News 3:26–37.

Skipper NT, Smalley MV, Williams GD, Soper AK, Thompson CH. 1995. Direct measurement of the electrical double-layer structure in hydrated lithium vermiculite clays by neutron diffraction. J Phys Chem 99:14201–14204.

Skipper NT, Soper AK, McConnell JDC. 1991. The structure of interlayer water in vermiculite. J Chem Phys 94:5751–5760.

Skipper NT, Soper AK, Smalley MV. 1994. Neutron diffraction study of calcium vermiculite: Hydration of calcium ions in a confined environment. J Phys Chem 98:942–945.

Skipper NT, Sposito G, Chang F-RC. 1995. Monte Carlo simulation of interlayer molecular structure in swelling clay minerals: 1. Methodology. Clays Clay Miner 43:285–293.

Slade PG, Quirk JP, Norrish K. 1991. Crystalline swelling of smectite samples in concentrated NaCl solutions in relation to layer charge. Clays Clay Miner 39:234–238.

Slade PG, Stone PA, Radoslovich EW. 1985. Interlayer structure of the two-layer hydrates of Na- and Ca- vermiculites. Clays Clay Miner 33:51–61.

Soper AK, Phillips MG. 1986. A new determination of the structure of water at 25°C. Chem Phys 107:47–60.

Sposito G, Prost R. 1982. Structure of water absorbed on smectites. Chem Rev 82:553–573.

(*Received 19 April 1996; accepted 3 July 1996; Ms. 2761*)